Royal Netherlands Institute for Sea Research

This is a postprint of:

Article begins on next page]

Chapter 4

Latitudinal variation in virus-induced mortality of phytoplankton across the North Atlantic Ocean

Kristina D. A. Mojica[1], Jef Huisman[2], Steven W. Wilhelm[3], and Corina P. D. Brussaard[1,2]

[1]Department of Biological Oceanography, Royal Netherlands Institute for Sea Research (NIOZ), P.O. Box 59, 1790 AB Den Burg, Texel, The Netherlands.
[2]Department of Aquatic Microbiology, Institute for Biodiversity and Ecosystem Dynamics (IBED), University of Amsterdam, P.O. Box 94248, 1090 GE Amsterdam, The Netherlands.
[3]Department of Microbiology, University of Tennessee, Knoxville, Tennessee 37996, USA.

Abstract

Viral lysis of phytoplankton constrains marine primary production, food web dynamics, and biogeochemical cycles in the ocean. Yet, little is known about the biogeographical distribution of viral lysis rates across the global ocean. To address this, we investigated phytoplankton group-specific viral lysis rates along a latitudinal gradient within the North Atlantic Ocean. The data show large-scale distribution patterns of different virus groups across the North Atlantic that are associated with the biogeographical distributions of their potential microbial hosts. Average virus-mediated lysis rates of the picocyanobacteria *Prochlorococcus* and *Synechococcus* were lower than those of the picoeukaryotic and nanoeukaryotic phytoplankton (i.e., 0.14 d^{-1} compared to 0.19 and 0.23 d^{-1}, respectively). Total phytoplankton mortality (virus plus grazer-mediated) was comparable to the gross growth rate, demonstrating high turnover rates of phytoplankton populations. Virus-induced mortality was an important loss process at low and mid latitudes whereas phytoplankton mortality was dominated by microzooplankton grazing at higher latitudes (> 56°N). This shift from a viral-lysis-dominated to a grazing-dominated phytoplankton community was associated with a decrease in temperature and salinity, and the decrease in viral lysis rates was also associated with increased vertical mixing at higher latitudes. Ocean-climate models predict that surface warming will lead to an expansion of the stratified and oligotrophic regions of the world's oceans. Our findings suggest that these future shifts in the regional climate of the ocean surface layer are likely to increase the contribution of viral lysis to phytoplankton mortality in the higher-latitude waters of the North Atlantic, which may potentially reduce transfer of matter and energy up the food chain and thus affect the capacity of the northern North Atlantic to act as a long-term sink for CO_2.

Introduction

Viruses are important mortality agents for marine phytoplankton (Evans et al. 2003; Brussaard 2004a; Tomaru et al. 2004; Baudoux et al. 2006). Through the lysis of their autotrophic hosts viruses regulate primary production (Suttle et al. 1990) and play key roles in species competition and succession of phytoplankton populations (Gobler et al. 1997; Mühling et al. 2005; Haaber and Middelboe 2009). Moreover, lysis of microbes diverts energy and biomass away from the classical grazer-mediated food web towards microbial-mediated recycling and the dissolved organic matter pool. This 'viral shunt' reduces the transfer of carbon and nutrients to higher trophic levels, while enhancing the recycling of potential growth-limiting nutrients (Fuhrman 1999; Wilhelm and Suttle 1999). In this manner, viruses have major effects on nutrient cycles and energy flow in the ocean (Brussaard and Martinez 2008; Weitz and Wilhelm 2012). As microbial photoautotrophs are responsible for roughly half of the global annual carbon dioxide fixation and sustain the higher trophic levels in marine ecosystems (Field et al. 1998), their viruses also have the potential to influence these global scale processes.

Marine virus dynamics and virus-host interactions are affected by both abiotic and biotic factors (Mojica and Brussaard 2014), which can vary on both spatial and temporal scales. However, despite biogeographical distributions of bacteria and phytoplankton being extensively studied (Irigoien et al. 2004; Martiny et al. 2006; Fuhrman et al. 2008), the possible existence of biogeographical patterns in marine viral populations (and how these may vary) has received less attention (Breitbart and Rohwer 2005; Angly et al. 2006; Matteson et al. 2013). For example, thermal stratification is an important factor regulating phytoplankton dynamics and ocean-climate models predict that global warming will lead to an expansion of the stratified regions of the world's oceans (Sarmiento et al. 1998; Toggweiler and Russell 2008). Projected alterations to stratification and vertical mixing have the potential to affect the species composition (Huisman et al. 2004; Mojica et al. 2015), phenology (Edwards and Richardson 2004), productivity (Gregg et al. 2003; Behrenfeld et al. 2006; Polovina et al. 2008), size structure (Daufresne et al. 2009; Hilligsøe et al. 2011), nutritional value (Mitra and Flynn 2005; van de Waal et al. 2010), abundance (Richardson and Schoeman 2004) and biogeographical distribution (Doney et al. 2012; Flombaum et al. 2013; van de Poll et al. 2013) of marine phytoplankton. As obligate parasites, viruses rely upon their host to provide the machinary, energy and resources required for viral replication and assembly.

4

Consequently, factors regulating the physiology, production and removal of the host are also important in governing viral dynamics (Van Etten et al. 1983; Moebus 1996; Baudoux and Brussaard 2008; Maat et al. 2014). Therefore, future changes in stratification also have the potential to affect the composition and distribution of viral assemblages associated with phytoplankton communities, and the sensitivity of marine phytoplankton populations to grazing and viral infection.

The North Atlantic Ocean offers a large-scale latitudinal gradient, with permanent stratification in the subtropics and seasonal stratification in the temperate zones (Longhurst 2007; Jurado et al. 2012). The spring phytoplankton bloom is triggered by reduced vertical mixing and the onset of seasonal stratification due to warming of the surface waters (Sverdrup 1953; Huisman et al. 1999; Taylor and Ferrari 2011), and represents one of the most important biological events in the North Atlantic (Siegel et al. 2002). The bloom begins in December–January at a latitude of ~35° N, just north of the permanently stratified waters of the North Atlantic Subtropical Gyre and subsequently spreads across the North Atlantic throughout spring and summer, expanding northwards to Arctic waters in June (Siegel et al. 2002). The spring bloom takes up large amounts of CO_2, and owing to deep water formation at high latitudes the North Atlantic plays a key role in oceanic CO_2 sequestration (Deser and Blackmon 1993). Yet, little is known about biogeographical patterns in viral abundances and viral lysis rates of phytoplankton across the North Atlantic, and how these may affect the transfer of the photosynthetically acquired carbon and energy to higher trophic levels. This is primarily due to a severe lack of quantitative estimates of phytoplankton losses due to viral lysis (Weitz and Wilhelm 2012), and how these relate to changes in environmental variables.

In this study, we therefore investigate large-scale distribution patterns of (i) marine viral groups and their potential hosts, and (ii) viral lysis and grazing rates of marine phytoplankton over a latitudinal gradient across the North Atlantic Ocean. Specifically, we assess the following hypotheses: (H1) The abundances and composition of the microbial host populations (i.e., bacteria and phytoplankton) vary with latitude (H1a), and are strongly affected by changes in water column stratification (H1b). (H2) The biogeographical distributions of the different viruses depend on the biogeographical distributions of their microbial host populations. (H3) Viral lysis rates of marine phytoplankton vary with latitude, affecting the relative importance of the viral shunt versus the classic grazing-mediated food web.

Materials and methods

Sampling and physicochemical variables

In July-August of 2009, 32 stations were sampled in the Northeast Atlantic Ocean during the shipboard expedition of STRATIPHYT (Changes in vertical stratification and its impacts on phytoplankton communities) (Figure 1). Water samples were collected from at least 10 separate depths in the top 250 m water column using GO-Flo, 10 liter samplers mounted on an ultra-clean (trace-metal free) system equipped with CTD (Seabird 9+) with standard sensors and auxiliary sensors for chlorophyll autofluorescence (Chelsea Aquatracka Mk III). Data from the chlorophyll autofluorescence sensor were calibrated against HPLC data according to van de Poll et al. (2013) in order to determine total Chlorophyll *a* (Chl *a*). Samples were taken inside a 6 m clean lab for analysis of inorganic nutrients (5 ml) and flow cytometry (10 ml). Samples for dissolved inorganic nutrients (5 ml) were analyzed onboard using a Bran+Luebbe Quaatro AutoAnalyzer for dissolved orthophosphate (Murphy and Riley 1962), nitrate and nitrite (NO_x) (Grasshoff, 1983) and ammonium (Koroleff 1969; Helder and de Vries 1979). Detection limits were 0.028 µmol L^{-1} for PO_4^{3-}, 0.10 µmol L^{-1} for NO_x, and 0.09 µmol $L^{-1}$for NH_4^+. Water samples for the modified dilution assay, to determine viral lysis and microzooplankton grazing rates on phytoplankton, were taken from the depth with maximal phytoplankton Chl *a* autofluorescence, i.e., the deep chlorophyll maximum (DCM) or mixed layer (ML). All materials used for sampling water for dilution experiments were prewashed in acid (0.1 M HCl, overnight), rinsed with Milli-Q water (3 times) and rinsed with *in situ* water before use.

Density of seawater was expressed as sigma-t (σ_T) values, defined as $\sigma_T = \rho(S,T)$ - 1000, where $\rho(S,T)$ is the density of seawater at temperature *T* and salinity *S* measured in kg m^{-3} at standard atmospheric pressure. Temperature eddy diffusivity (K_T) data, referred to here as the vertical mixing coefficient, were derived from temperature and conductivity microstructure profiles measured using a SCAMP (Self Contained Autonomous Microprofiler) (Stevens et al. 1999; Jurado et al. 2012). The SCAMP was deployed at fewer stations (i.e., 14) and to lower depths (up to 100 m) than the remainder of the data in the present study. In order to correct for this deficiency, data were interpolated using the spatial kriging function 'krig' executed in R using the 'fields' package (Furrer et al. 2012). Interpolated K_T values were bounded below by the minimum value measured; the upper values were left unbounded. This resulted in estimated K_T values which preserved the

4

qualitative pattern and range of values previously reported (Jurado et al. 2012). In addition, the depth of the mixed layer (Z_m) was determined as the depth at which the temperature difference with respect to the surface was 0.5°C (Levitus et al. 2000; Jurado et al. 2012). As shown by Brainerd and Gregg (1995), this definition of the mixed layer provides an estimate of the depth through which surface waters have been mixed in recent days. On the few occasions where SCAMP data were not available, Z_m was determined from CTD data. Temperature profiles obtained from SCAMP and CTD measurements were compared and showed good agreement. To quantify the strength of stratification, CTD data was processed with SBE Seabird software to calculate the Brunt-Väisälä frequency (N^2, in $rad^2 s^{-2}$) using the Fofonoff adiabatic leveling method (Bray and Fofonoff 1981). The Brunt-Väisälä frequency represents the angular velocity (i.e., the rate) at which a small perturbation of the stratification will re-equilibrate. Hence, it is a simple measure of the stability of the vertical stratification.
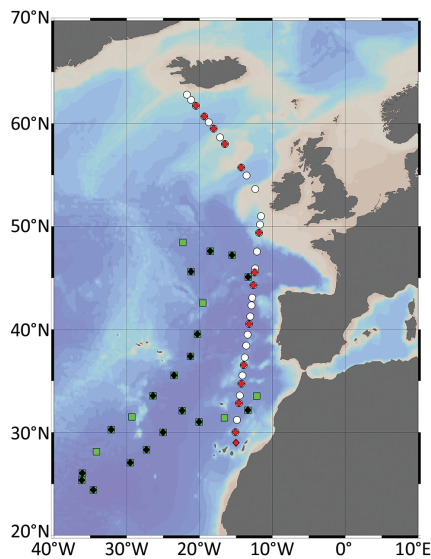
Figure 1. Bathymetric map of the stations sampled during the cruises STRATIPHYT (white circles and red diamonds) and MEDEA (green squares and black diamonds). Modified dilution assays to determine viral lysis and microzooplankton grazing rates were performed at stations indicated by the red and black diamonds. Cruise track was prepared using Ocean Data View (ODV version 4.6.5, Schlitzer, 2002).

In October-November 2011, an opportunity was presented to join the MEDEA (Microbial Ecology of the Deep Atlantic) cruise, to conduct additional modified dilution experiments in the oligotrophic area of the Northeast Atlantic Ocean

(Figure 1). During MEDEA, physicochemical parameters were measured from 3-5 depths per station within the upper 120 m water column using the same methods as for STRATIPHYT. However, no SCAMP measurements were conducted during MEDEA, and ammonium concentrations were not determined. Samples for modified dilution assays were taken mostly from the DCM depth (Table S1).

Microbial abundances

Viruses, bacteria, cyanobacteria and eukaryotic phytoplankton < 20 μm were enumerated using a Becton-Dickinson FACSCalibur flow cytometer (FCM) equipped with an air-cooled Argon laser with an excitation wavelength of 488 nm (15 mW). Approximately 1 ml of fresh seawater was used for enumeration of phytoplankton using methods described by Marie et al. (2005). Phytoplankton were differentiated based on their auto-fluorescence properties using bivariate scatter plots of either orange (i.e., phycoerythrin, present in *Synechococcus* spp.) or red fluorescence (i.e., chlorophyll *a*, present in all phytoplankton) against side scatter. Average cell size for phytoplankton subpopulations were determined by size-fractionation of whole water by sequential gravity filtration through 8, 5, 3, 2, 1, 0.8, and 0.4 *μ*m pore-size polycarbonate filters, by assuming spherical diameter (Ø) of size displayed by the median (50%) number of cells retained for that cluster. In total, eight distinct phytoplankton groups were detected and sized by sequential size-fractioned gravity filtration, i.e., 2 picoeukaryotic groups (average Ø of 1.4 and 1.5 μm, respectively), 3 nanoeukaryotic groups (3, 6 and 8 μm Ø, respectively), and 3 picocyanobacteria groups (*Synechococcus* spp. of 0.9 μm Ø, and ecotypes *Prochlorococcus* high-light (HL) of 0.6 μm Ø in surface waters and *Prochlorococcus* low-light (LL) of 0.7 μm Ø in the DCM).

Bacteria and viruses were enumerated according to Marie et al. (1999) and Brussaard et al. (2010), respectively, with modifications according to Mojica et al. (2014). Briefly, samples were fixed with 25% glutaraldehyde (EM-grade, Sigma-Aldrich, Netherlands) to a final concentration of 0.5% for 15-30 min at 4 °C, flash frozen and stored at -80 °C until analysis. Thawed samples were diluted in TE buffer (pH 8.2, 10 mM Tris-HCL, 1 mM EDTA; Mojica *et al.*, 2014), stained with the nucleic acid-specific green fluorescence dye SYBR Green I (final concentration of 1 x 10^{-4} and 5 x 10^{-5} of the commercial stock concentration; Life Technologies, Netherlands) and incubated in the dark at either room temperature for 15 min or at 80 °C for 10 min, for bacteria and viruses, respectively. Cooled samples (5 min, room temperature) were then analyzed on the flow cytometer with the

discriminator set on green fluorescence. Five distinct virus groups, labeled V1-V5, were identified based on their green fluorescence and side scatter characteristics (Figure 2). Low fluorescing viral groups, V1 and V2, are considered to be primarily dominated by phages infecting heterotrophic bacteria, although some evidence suggests that eukaryotic algal viruses can also display similar low fluorescence signatures (Brussaard and Martinez 2008; Brussaard et al. 2010). The other virus groups generally contain more algal viruses, with both pro- and eukaryotic algal viruses contributing to the V3 group, while the higher side scatter groups, V4 and V5, commonly represent large dsDNA algal viruses (Jacquet et al. 2002; Brussaard 2004b; Baudoux et al. 2006).
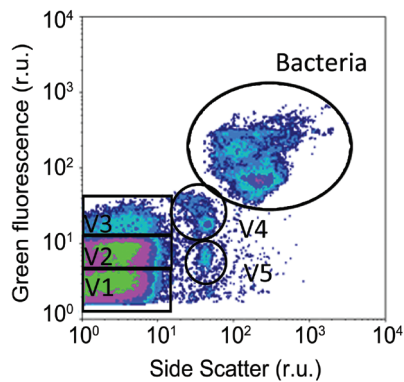
Figure 2. A typical dot plot of viruses counted with flow cytometry in a sample of the STRATIPHYT cruise. Viruses (and bacteria)were discriminated by green fluorescence versus side scatter; V1-V5 indicate the 5 virus groups distinguished by flow cytometry.

Redundancy analysis

We applied multivariate statistical analysis to data obtained from STRATIPHYT to test hypotheses (H1) and (H2) put forth in the Introduction. The analysis was performed using R statistical software (R Development Core Team, 2012) supplemented by the vegan package (Oksanen et al. 2013).

First, we performed a data exploration following the protocol described in Zuur et al. (2010). Most phytoplankton groups distinguished by flow cytometry had limited biogeographical distributions within our study area and consequently suffered from zero inflation (e.g., zeroes in > 20% of the data points for almost every phytoplankton group). To avoid issues arising from zero inflation and provide good quality explanatory data, phytoplankton groups were clustered into

different categories: total picocyanobacteria (*Synechococcus*, *Prochlorococcus* HL-ecotype and *Prochlorococcus* LL-ecotype), total picoeukaryotes (picoeukaryotes I+II), total nanoeukaryotes (nanoeukaryotes I+II+III), and total phytoplankton. For hypothesis (H1), the response variables were the abundances of the bacteria and different phytoplankton groups and total Chl *a*, while the explanatory variables were latitude, vertical mixing coefficient (K_T, temperature eddy diffusivity), a stratification index (N^2, Brunt Väisälä frequency), and temperature. For hypothesis (H2), the response variables were the virus groups V1-V5 and total viral abundance, while the explanatory variables were the bacteria, different phytoplankton groups, total Chl *a* and the environmental variables latitude, K_T, N^2, and temperature. Virus, bacteria, phytoplankton and chlorophyll data were log(x+1) transformed and the vertical mixing coefficient and temperature were log transformed to improve the homogeneity of variance.

Next, to obtain the most parsimonious model, data were examined for collinearity of the explanatory variables by calculating variance inflation factors (VIF) using the R function corvif (Zuur *et al.*, 2009). In a stepwise fashion, all explanatory variables with VIF > 8 were removed from the model. For hypothesis (H1), VIF analysis resulted in the selection of 4 explanatory variables: latitude, K_T, N^2 and temperature. For hypothesis (H2), VIF analysis resulted in the selection of 8 explanatory variables: picocyanobacteria (Cyano), picoeukaryotic phytoplankton (PicoEUK), nanoeukaryotic phytoplankton (NanoEUK), bacteria, Chl *a*, latitude, N^2, K_T and temperature.

Initial scatterplots of the response and explanatory variables revealed strong linear relationships and therefore redundancy analysis (RDA) (Zuur et al. 2009) was chosen over canonical correspondence analysis (CCA). RDA is a combination of multiple regression analysis and principal component analysis for multivariate data. Forward selection was applied to select only those explanatory variables that contributed significantly to the RDA model, while removing non-significant terms. Significance was assessed by a permutation test, using the multivariate pseudo-F as test statistic (Zuur et al. 2009). A total of 9,999 permutations were used to estimate *p*-values associated with the pseudo-F statistic.

RDA was based on all sampling points for which we had a complete dataset of explanatory and response variables. For hypothesis (H1), this amounted to 80 samples (ranging from 0-225 m depth, with 4-11 depths sampled per station) from 15 stations of the STRATIPHYT cruise. For hypothesis (H2), the explanatory variable N^2 was not significant (see *Results*). Hence, RDA could be performed on

4

96 samples, as the removal of N^2 permitted the inclusion of sampling points from STRATIPHYT stations that lacked N^2 data.

Modified dilution experiments

To investigate hypothesis (H3) we determined viral lysis and microzooplankton grazing rates of the different phytoplankton groups using the modified dilution assay according to Kimmance and Brussaard (2010). For both the STRATIPHYT and MEDEA cruises, experiments were conducted onboard, using water samples obtained from those depths where Chl *a* autofluorescence was maximal (i.e., DCM or ML). Natural seawater, gently passed through a 200 µm mesh to remove mesozooplankton (while retaining microzooplankton), was combined with 0.45 µm diluent or 30 kDa ultrafiltrate in proportions of 100, 70, 40 and 20% to gradually decrease the mortality impact with increasing dilution (Figure S1a). The 0.45 µm filtrate, prepared with the goal of removing the microzooplankton grazers, was achieved by gravity filtration of natural seawater through a 0.45 µm Sartopore capsule filter with a 0.8 µm prefilter (Sartopore 2 300, Sartorius stedim biotech). The 30 kDa ultrafiltrate, prepared to remove grazers and viruses, was generated by tangential flow filtration using a polyethersulfone membrane (Vivaflow 200, Vivascience). All experiments were performed in triplicate in 1 L clear polycarbonate bottles. After preparation of the two parallel dilution series (12 bottles each), a 3 ml subsample was taken and phytoplankton was enumerated by FCM as specified previously. The bottles were then incubated for 24 hours in an on-deck flow-through seawater incubator at *in situ* temperature and light (using neutral density screen) conditions. After the 24-hour incubation period, a second FCM phytoplankton count was executed and the resulting growth rate for each phytoplankton group determined. Dual measurements of viral lysis and grazing rates were obtained for all phytoplankton groups, except for *Prochlorococcus* HL which was largely absent from the sampled depths.

The microzooplankton grazing rate was estimated from the regression coefficient of the apparent growth rate versus fraction of natural seawater for the 0.45 µm series, while the combined rate of viral-induced lysis and microzooplankton grazing was estimated from a similar regression for the 30 kDa series (Figure S1b and c) (Baudoux et al. 2006; Kimmance and Brussaard 2010). A significant difference between the two regression coefficients (as tested by ANCOVA) indicates a significant viral lysis rate. Phytoplankton gross growth rate (μ_{gross}, in the absence of grazing and viral lysis) was derived from the y intercept of the 30 kDa series regression.

The viral lysis and grazing rates were analyzed with a two-way analysis of variance with type II sum of squares to assess differences between the two sources of mortality (viral lysis versus grazing) and among the phytoplankton groups (*Synechococcus*, *Prochlorococcus* LL, total picoeukaryotes and total nanoeukaryotes). Homogeneity of variance was confirmed by Levene's test, and post-hoc comparison of the means was based on Tukey's HSD test using SPSS version 22.0. Potential relationships between biological parameters obtained from the modified dilution assays (e.g., phytoplankton abundance, μ_{gross}, viral lysis and grazing rates) and environmental parameters were examined by Spearman's rank correlation coefficient. Probability values were adjusted with Holm's correction for multiple hypothesis testing using the corr.p function of psych (Revelle 2014) implemented in R (R Development Core Team 2012). The correlation analysis was performed on the complete data set (n = 105) with a significance level (α) of 0.05.

Results

During both the STRATIPHYT and MEDEA cruise, the North Atlantic was characterized by a strong temperature-induced vertical stratification resulting in very low concentrations of dissolved inorganic nitrogen and phosphorus in the upper 50-100 m water column at latitudes south of 45°N (Figure 3a-g; Figure S2). Towards the north stratification weakened, slightly relaxing nutrient limitation in the upper 50 m surface layer.

For both cruises, pico-sized phytoplankton (< 2 μm Ø) accounted for more than 95% of the total phytoplankton < 20 μm enumerated by FCM. South of 45°N, both total phytoplankton abundance (up to $1.6 \pm 0.4 \times 10^5$ cells ml^{-1}) and Chl *a* (Figure 3g; Figure S2e) were maximal between 30 and 100 m depth, characteristic of a deep-chlorophyll maximum (DCM). Cyanobacteria were the most abundant members of the phytoplankton community in this southern region (Figure 4a), and consisted mainly of *Prochlorococcus*-HL and *Prochlorococcus*-LL (Figure S3a and b). The DCM shallowed with latitude, giving over to a surface maximum north of 45°N, marking the northern boundary of the oligotrophic areas (defined by Chl *a* concentrations < 0.07 mg Chl m^{-3}; Polovina et al. 2008). Cyanobacterial abundance decreased with the loss of the DCM and disappearance of *Prochlorococcus* spp. north of 45°N (Figure 4a, Figure S3a and b). However, the cyanobacteria *Synechococcus* spp. showed highest abundances in the most northern stations, beyond 56°N, where

they numerically dominated the photosynthetic community < 20 µm (Figure S3c). Picoeukaryotic and nanoeukaryotic phytoplankton were relatively abundant in the DCM between 38°N and 45°N, and reached maximal abundances in the surface waters of the stations north of 54°N (Figure 4b and c, Figure S3d-h). Bacterial abundance was maximal in the surface waters of the most northern stations (Figure 4d).
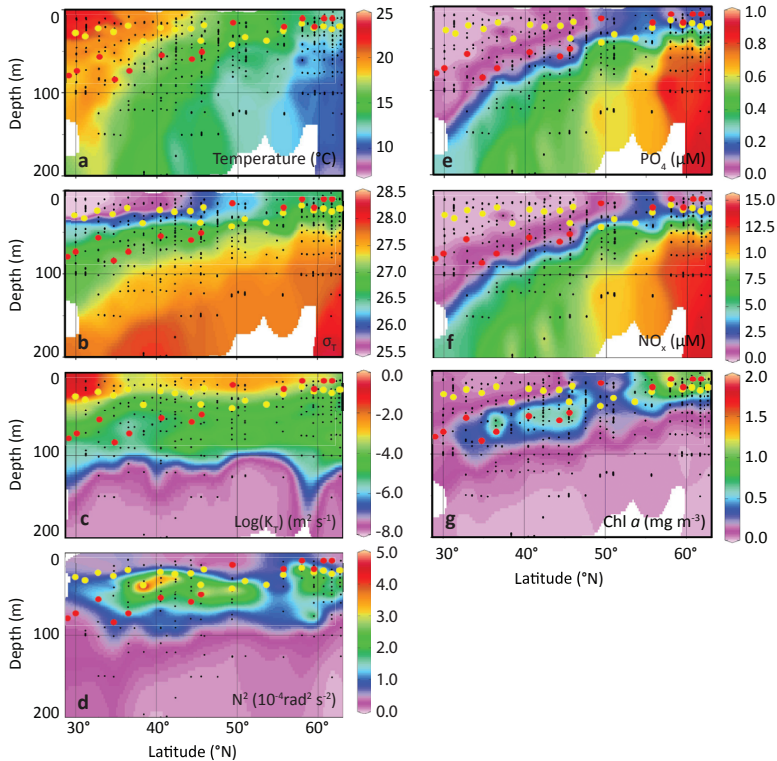
Figure 3. Latitudinal and depth distribution of (a) temperature, (b) sigma-t (σ_T), (c) Temperature eddy diffusivity (K_T), (d) Brunt-Väisälä frequency (N^2), (e) inorganic phosphorus, (f) NO_x (nitrate + nitrite) and (g) Chl a concentrations measured during STRATIPHYT. Black dots indicate sampling points, yellow dots indicate mixed layer depth (Z_m), and red dots the sampling depths for modified dilution assays. Figure panels were prepared using Ocean Data View (ODV version 4.6.5, Schlitzer, 2002).

The 5 virus groups showed distinct biogeographical distributions (Figure 4e-i). Although V1 and V2 viruses were the numerically dominant virus groups in the DCM of the strongly stratified waters below 45°N, they were even more abundant in the top 50 m of the weakly stratified waters at latitudes above 45°N (Figure 4e and f). Conversely, V3 viruses reached their highest abundances between 30-100

m depth in the DCM of stratified waters south of 45°N (Figure 4g). V4 and V5 viruses were present throughout the latitudinal range, but V4 reached its maximum abundance in the subsurface waters located between latitudes 40-45°N (Figure 4h) and V5 had its highest abundance in the upper 50 m surface waters in the weakly stratified waters at the higher latitudes (Figure 4i).
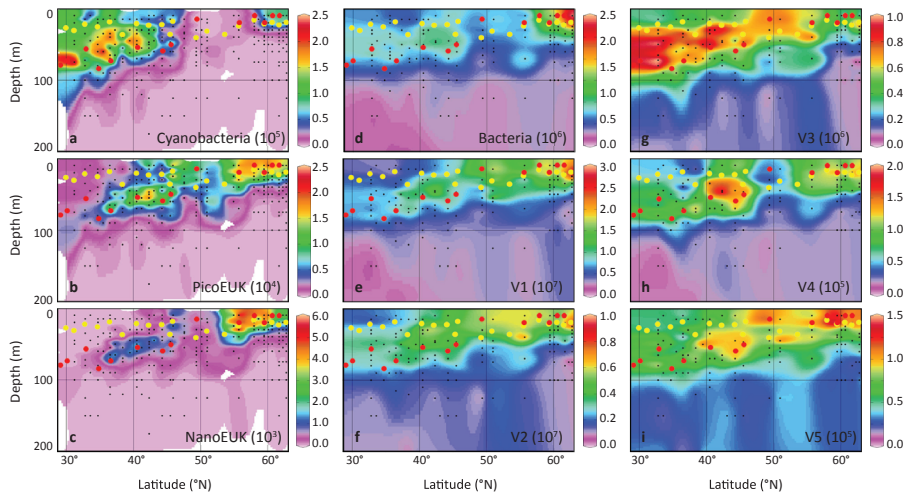
Figure 4. Biogeographical distributions of phytoplankton (a-c), bacteria (d) and virus groups (e-i) across the Northeast Atlantic Ocean based on flow cytometry counts obtained during the STRATIPHYT cruise. Abundances are expressed in (a-c) cells ml^{-1}, (d) bacteria ml^{-1} and (e-i) viruses ml^{-1}. Black dots indicate sampling points, yellow dots indicate mixed layer depth (Z_m), and red dots the sampling depths for modified dilution assays. Graphs were prepared with Ocean Data View (ODV version 4.6.5, Schlitzer, 2002).

The hypothesis (H1) that abundances and composition of the microbial host populations (e.g., bacteria and phytoplankton) vary with latitude (H1a), and are strongly affected by changes in water column stratification (H1b) is confirmed by the RDA results. Forward selection revealed that latitude and the stratification variables K_T, N^2 and temperature all contributed significantly to the RDA model (Table 1). The results are presented in a RDA triplot (Figure 5a). The first two axes in the RDA triplot explained 27% and 4% of the variation in the data. The concentrations of bacteria, cyanobacteria, picoeukaryotic and nanoeukaryotic phytoplankton were all positively correlated with K_T and N^2. The strong positive correlation between picoeukaryotes and N^2 is particularly noteworthy, indicating that picoeukaryotes reached their highest concentrations at or near the pycnocline. In comparison to the other species groups, cyanobacteria showed a relatively strong

correlation with temperature and nanoeukaryotes a relatively strong correlation with latitude.

Table 1. Significance of the selected explanatory variables in the RDA correlation triplots (see Figure 5a and b).

Explanatory variable	AIC*	Pseudo-F	P
Host populations (H1)			
K_T	103.5	33	0.005
Temperature	95.4	10.4	0.005
Latitude	79.7	18.9	0.005
N^2	71.1	10.6	0.005
Virus populations (H2)			
Bacteria	89.5	135.0	0.005
PicoEUK	71.7	21.4	0.005
NanoEUK	64.8	8.9	0.005
Temperature	58.5	8.3	0.005
Cyano	54.1	6.1	0.005
Latitude	52.9	3.1	0.025

Footnote: AIC = Akaike Information Criterion. The explanatory variables were selected by forward selection based on the pseudo-F statistic, using 9,999 permutations to assess their significance. Total variation explained by the RDA models was 57 and 75%, respectively.

RDA was also applied to investigate hypothesis (H2) that the biogeographical distributions of the viruses depend on the biogeographical distributions of their hosts. Forward selection revealed that latitude, temperature and the four different potential host groups contributed significantly to the RDA model (Table 1), whereas the environmental variables K_T, Chl a and N^2 (pseudo-F = 1.1, 0.8, and 0.2; $p = 0.39$, 0.53, and 0.91, respectively) did not. The first two axes of the RDA triplot (Figure 5b) explained 51% and 3% of the variation in the data. In line with expectation, the RDA triplot shows that the biogeographical distribution of V1 viruses was tightly coupled to the distribution of total bacterial abundance (Figure 5b).The distribution of V2 viruses was correlated with total picoeukaryotic phytoplankton abundance, while the distribution of V3 viruses was strongly correlated with total picocyanobacterial abundance. Furthermore, distributions of V4 and V5 viruses were associated with high abundances of nanoeukaryotic phytoplankton and bacteria (Figure 5b).
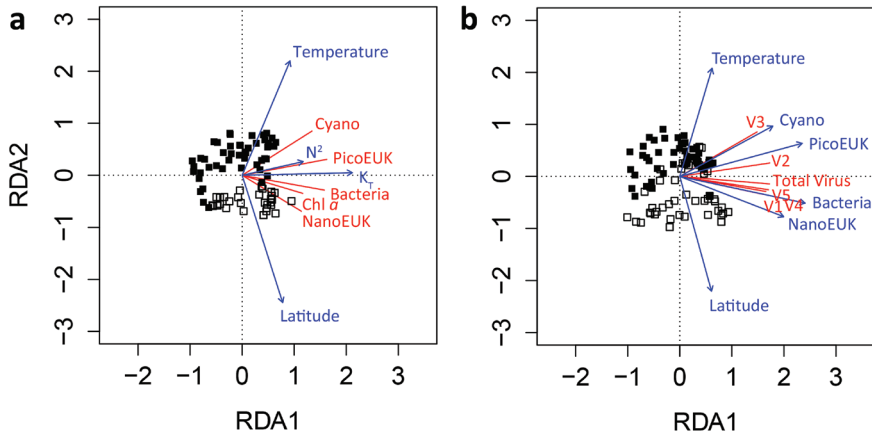
Figure 5. Redundancy Analysis (RDA) correlation triplot describing (**a**) the biogeographical distribution of potential microbial hosts (response variables, in red) in relation to environmental variables relevant to stratification (explanatory variables, in blue) and (**b**) the biogeographical distributions of the viruses (response variables, in red) in relation to latitude and the biogeographical distributions of their hosts (explanatory variables, in blue) using data obtained during the STRATIPHYT cruise. Symbols represent individual sampling points (n = 80 and 96 in panels a and b, respectively), where closed squares represent sampling points at stations with a deep chlorophyll maximum (DCM) and open squares represent sampling points at stations without a DCM. The DCM was defined by the presence of a subsurface peak in the vertical profile of Chl a autofluorescence, which is a common feature of vertically stratified oligotrophic waters. All explanatory variables in the triplot are significant (Table 1). Total variation explained by the RDA models in panels a and b were 57 and 75%, respectively.

To assess hypothesis (H3), we quantified the contributions of viral lysis and grazing to the mortality of the different phytoplankton groups by conducting 34 modified dilution assays across the North Atlantic during the two cruises (Figure 1; see Tables S1 and S2 for details). We first tested whether the modified dilution assays themselves had any undesirable side effects on phytoplankton performance. In general, we found no associated reduction in growth rate for any of the phytoplankton groups in the 20% fraction of the 30Ka series, where potential enhanced nutrient limitation would be greatest due to reduced remineralization (as a result of removal of bacteria and grazers). Furthermore, the photosynthetic capacity remained high for all dilutions (Fv/Fm = 0.6).

Viral lysis rates varied from 0 to 1.05 d^{-1} (Table S2). Two-way analysis of variance of the mortality rates revealed a significant main effect of the phytoplankton groups ($F_{3,188}$ = 4.761; p = 0.003), while the main effect of the mortality source (grazing vs viral lysis) ($F_{1,188}$ = 2.316; p > 0.05) and the interaction term ($F_{3,188}$ = 0.115; p > 0.05) were both non-significant. In other words, viral lysis rates were comparable to microzooplankton grazing rates for all phytoplankton groups measured (Figure

6), demonstrating that virus-mediated lysis contributed to approximately half of the total phytoplankton mortality. However, mortality rates differed between the phytoplankton groups. The mortality rates of nanoeukaryotic and picoeukaryotic phytoplankton were not significantly different, and these two groups demonstrated the highest average viral lysis rates of 0.23 and 0.19 d^{-1} and grazing rates of 0.27 and 0.21 d^{-1}, respectively (Figure 6). *Synechococcus* and *Prochlorococcus* experienced significantly lower mortality rates compared to the nanoeukaryotes, with viral lysis rates of 0.14 d^{-1} and grazing rates of 0.13 d^{-1}.
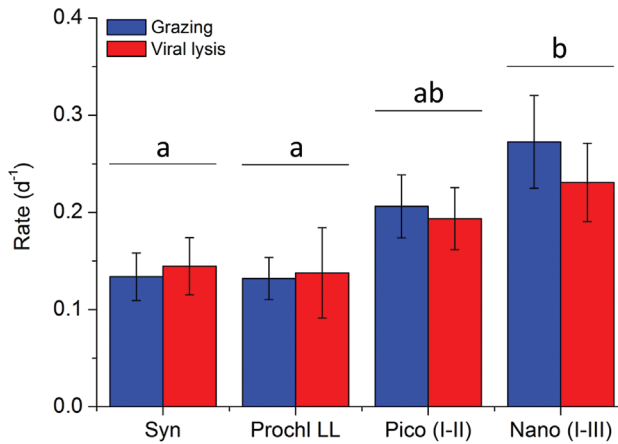
Figure 6. Grazing and viral lysis rates of the different phytoplankton groups. Grazing and viral lysis rates were determined using the modified dilution assay. The phytoplankton groups include Synechococcus (Syn, sample size N = 19), low-light adapted Prochlorococcus (Prochl LL, N = 13), picoeukaryotes (Pico I-II, N = 45), and nanoeukaryotes (Nano I-III, N = 28). High-light adapted Prochlorococcus was largely absent at the depths sampled for the modified dilution assays. Error bars represent standard error. Bars with different letters are significantly different (p<0.05), as tested by two-way analysis of variance followed by post hoc comparison of the means using Tukey's HSD.

Total mortality rates of the specific phytoplankton groups ranged from 0.01 to 1.20 d^{-1}, and were in balance with gross growth rates (Figure 7a), emphasizing fast turnover of the photoautotrophic production. Moreover, our data show a remarkable reduction in the ratio of viral lysis rates to microzooplankton grazing rates (V:G) at higher latitudes (> 56°N)(Figure 7b). This switch from a viral lysis-dominated to a grazing-dominated plankton community was consistent across different phytoplankton groups (Figure 7b). The pattern is corroborated by a significant negative correlation of V:G with latitude and a significant positive correlation with temperature and salinity (Table 2). Similarly, viral lysis rates but not the grazing rates showed a significant negative correlation with latitude and K_T and positive

correlation with temperature and salinity, suggesting that the reduction in V:G was due to decreased viral lysis rates at higher latitudes (Table 2).
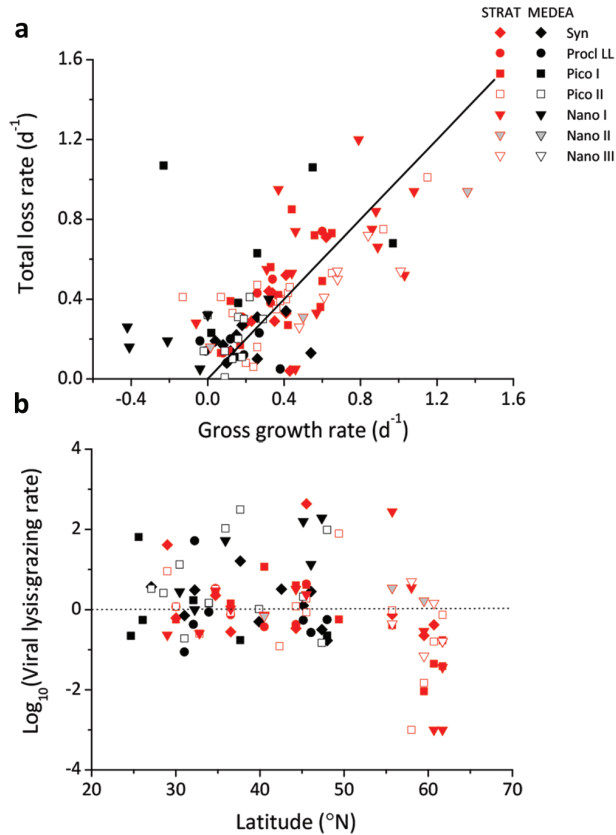
Figure 7. The contribution of viral lysis to phytoplankton mortality. (a) Relationship between the total loss rate (grazing + viral lysis) and gross growth rate of the 7 phytoplankton groups (< 20 μm). The black line indicates a 1:1 relationship. (b) Ratio of viral lysis to microzooplankton grazing rates for each of the 7 phytoplankton groups (< 20 μm) distinguished by flow cytometry, as function of latitude. Rates were obtained by the modified dilution technique during the STRATIPHYT (red symbols) and MEDEA (black symbols) cruises. High-light adapted Prochlorococcus were not included as they were largely absent at the depths sampled for the modified dilution assays. Dotted line indicates a 1:1 relationship of viral lysis to grazing.

Table 2. Spearman rank correlation coefficients (above the diagonal) and associated p-values (below the diagonal, with significant values highlighted in bold) of environmental and biological data obtained from modified dilution assays conducted during the STRATIPHYT and MEDEA cruises (N=105). Abbreviations represent phytoplankton host abundance (P0), gross growth rate (μgross), grazing rate (G), viral lysis rate (V), total mortality rate (TM) and the ratio of viral lysis to grazing rate (V:G).

	Latitude	Temperature	Salinity	sigma-t	K_T	N^2	PO_4	NO_x	P_0	μ_{gross}	G	V	T_M	V:G
Latitude		-0.95	-0.96	-0.67	0.68	n.s.	0.76	0.57	n.s.	n.s.	n.s.	-0.47	n.s.	-0.47
Temperature	**0.00**		0.89	0.56	-0.66	n.s.	-0.79	-0.61	n.s.	n.s.	n.s.	0.39	n.s.	0.41
Salinity	**0.00**	**0.00**		0.72	-0.65	n.s.	-0.77	-0.57	n.s.	n.s.	n.s.	0.45	n.s.	0.47
sigma-t	**0.00**	**0.00**	**0.00**		-0.76	n.s.	-0.65	-0.44	n.s.	n.s.	n.s.	0.48	n.s.	0.36
K_T	**0.00**	**0.00**	**0.00**	**0.00**		n.s.	0.63	0.43	n.s.	n.s.	n.s.	-0.43	n.s.	n.s.
N^2	1.00	1.00	1.00	1.00	0.34		n.s.	n.s.	n.s.	n.s.	n.s.	n.s.	n.s.	n.s.
PO_4	**0.00**	**0.00**	**0.00**	**0.00**	**0.00**	1.00		0.89	n.s.	n.s.	n.s.	n.s.	n.s.	n.s.
NO_x	**0.00**	**0.00**	**0.00**	**0.00**	**0.00**	1.00	**0.00**		n.s.	n.s.	n.s.	n.s.	n.s.	n.s.
P_0	1.00	1.00	1.00	1.00	1.00	1.00	1.00	1.00		-0.51	n.s.	n.s.	-0.38	n.s.
μ_{gross}	1.00	1.00	1.00	1.00	1.00	0.54	1.00	1.00	**0.00**		0.43	n.s.	0.64	n.s.
G	0.94	1.00	0.28	1.00	1.00	1.00	0.70	1.00	1.00	**0.00**		n.s.	0.67	-0.68
V	**0.00**	**0.00**	**0.00**	**0.00**	**0.00**	1.00	0.41	1.00	0.36	0.40	**0.00**		0.48	0.76
T_M	1.00	1.00	1.00	1.00	1.00	1.00	1.00	1.00	**0.00**	**0.00**	**0.00**	**0.00**		n.s.
V:G	**0.00**	**0.00**	**0.00**	**0.01**	0.11	1.00	0.22	1.00	**0.00**	**0.00**	**0.00**	**0.00**	1.00	

n.s. indicates non-significance at α = 0.05

Discussion

Our results demonstrate distinct biogeographical distributions of different virus groups and their potential host microbial populations across the North Atlantic Ocean (Figure 4). Metagenomic analyses of marine viral assemblages suggest that most viruses are widely dispersed across different oceanic regions (Angly et al. 2006), providing a seeding community for recruitment once the environmental conditions turn favorable (Breitbart and Rohwer 2005; Suttle 2007; Thingstad et al. 2014). Therefore, the classical tenet of 'all microbes are everywhere, but the environment selects' (Baas Becking 1931; de Wit and Bouvier 2006) is likely to apply to marine viruses. Accordingly, large-scale biogeographical variation in viral composition across the oceans is probably not caused by dispersal limitation but largely due to spatial variation in environmental conditions (Figure 5a). In particular, in agreement with hypothesis (H1) and (H2), our results show that the observed biogeographical distributions of marine viruses across the North Atlantic are strongly associated with the distributions of bacteria and phytoplankton that serve as their main hosts (Figure 5b). The large-scale distributions of these host species are in turn dependent on the latitudinal gradient from warm permanently stratified waters in the subtropical North Atlantic to colder seasonally stratified waters at higher latitudes (Figure 5a).

Yang et al. (2010) described a correlation between V3 viruses and picophytoplankton (including picocyanobacteria and picoeukaryotes) in the Pacific Ocean, with highest V3 virus abundances in tropical and subtropical waters. Our results show that the distribution of V3 viruses is closely related to the distribution of picocyanobacteria (*Prochlorococcus* and *Synechococcus*) (Figure 5b), indicating that the cluster of V3 viruses contains many cyanophages, which is in line with previous observations that cyanophages are particularly widespread in the (sub)tropical oceans (Suttle and Chan 1994; Wilson et al. 1999; Angly et al. 2006). In contrast, the distribution of V2 viruses appears to be linked to picoeukaryotic phytoplankton, and both the V2 viruses and picoeukaryotic phytoplankton are abundant at mid and high latitudes (Figure 4b, f and Figure 5b). Furthermore, our observation that V4 and V5 viruses are correlated to nanoeukaryotic phytoplankton (Figure 5b) corroborates earlier studies documenting similar FCM signatures for viruses infective against haptophytes (Jacquet et al. 2002; Brussaard 2004b; Baudoux et al. 2006).

The fate of primary production has important implications for the ecology and biogeochemical recycling of marine food webs. Estimates of viral lysis rates

of natural phytoplankton populations remain scarce, and consequently the importance of viruses in comparison to other loss factors remains unclear. Rates of viral-mediated mortality for *Synechococcus* (i.e., 0.03 - 0.49 d^{-1}), picoeukaryotic phytoplankton (i.e., 0 - 0.81 d^{-1}) and nanoeukaryotic phytoplankton (i.e., 0 - 1.05 d^{-1}) were comparable to the ranges reported in the literature (Baudoux et al. 2007, 2008; Evans and Brussaard 2012; Tsai et al. 2012). The viral lysis rates of *Prochlorococcus* (i.e., 0.02 - 0.57 d^{-1}) presented here were higher than the maximal 0.06 d^{-1} reported thus far (Baudoux et al. 2007). The typical set-up of the modified dilution assay (i.e., 2 parallel series, 4 dilutions, 3 replicates) lacks the sensitivity required to detect significance of viral lysis rates when rates are very low (Evans et al. 2003; Kimmance et al. 2007; Baudoux et al. 2008). Hence, we note that estimates of viral lysis rates < 0.1 d^{-1} should be interpreted with caution. To improve sensitivity of the method at low viral lysis rates, more replicates should be used.

Among the different phytoplankton groups, *Synechococcus* and *Prochlorococcus* experienced the lowest average viral lysis rates (i.e., 0.14 d^{-1}) (Figure 6). Considering the dominance of cyanophages and their hosts, the low viral mortality may seem surprising (Suttle and Chan 1993; Wang et al. 2011). However, *Synechococcus* and *Prochlorococcus* populations display high genotypic diversity and have the ability to develop resistance against viral infection (Waterbury and Valois 1993; Scanlan and West 2002), which could potentially reduce the impact of viral-induced mortality of these phytoplankton groups.

Virus-mediated lysis was responsible for approximately half of the total phytoplankton mortality in all four phytoplankton groups that we investigated, and comparable in magnitude to the mortality rate exerted by microzooplankton grazing (Figure 6). Total mortality of phytoplankton populations was in balance with gross growth (Figure 7a), indicating fast turnover of the photoautotrophic production within the North Atlantic Ocean. These results emphasize the need for the incorporation of viral lysis into ecosystems models (Franks 2001; Keller and Hood 2011; Keller and Hood 2013). Moreover, our results support hypothesis (H3) that viral lysis rates vary with latitude, and point at a striking reduction in the ratio of viral lysis rates to grazing rates of marine phytoplankton at higher latitudes (Figure 7b). While this observation might be a local or seasonal phenomenon, our findings are consistent with a smaller-scale study in the North Sea (Baudoux et al. 2008), which reported low viral lysis rates of picophytoplankton in offshore waters above 55°N. Furthermore, data from the Southern Ocean point at low viral lysis rates of phytoplankton over a relatively broad geographic range from at least 43°S

to 70°S on the southern hemisphere (Evans and Brussaard 2012). This suggests that low viral lysis rates at higher latitudes are not unique for our data set, but may represent a global pattern.

The underlying causes for the reduction in viral lysis rates with latitude remain unclear. Our results reveal a positive relationship between temperature and viral lysis rates of marine phytoplankton. While temperature has been shown to regulate viral infection of marine phytoplankton (Cottrell and Suttle 1995; Nagasaki and Yamaguchi 1998), evidence that temperature affects viral production rates is thus far largely restricted to bacterial hosts (Matteson et al. 2012; Mojica and Brussaard 2014). Vertical stratification represses turbulence and reduces mixed layer depth, thereby determining the general availability of light and nutrients to phytoplankton in the ocean (Behrenfeld et al. 2006; Huisman et al. 2006). These factors have been shown to be important factors regulating the production of viruses in phytoplankton hosts (Van Etten et al. 1983; Bratbak et al. 1998; Jacquet et al. 2002; Maat et al. 2014). Yet, we did not find a significant association between viral lysis rates and nutrient concentrations, host abundance or growth rate in our data (Table 2). In addition, viral lysis rates declined with latitude despite the latitudinal increase in total virus abundance as well as increases in V1 and V2 viruses (Figure 4; Table S3). An exception is the decline of the V3 viruses with latitude (Figure 4g; Table S3), which was due to the dominance of their picocyanobacterial hosts in the (sub) tropical southern region. Metagenomic analysis has revealed that lysogeny and prophage-like sequences are common in the Arctic Ocean (Angly et al. 2006). If this is a more general feature at higher latitudes, it may reduce the lytic viral lysis rates measured by the dilution assay. However, evidence for lysogeny in photoautotrophs is mostly restricted to prokaryotes (Paul 2008). Consequently, lysogeny would not fully explain the low viral lysis rates at higher latitudes for eukaryotic phytoplankton populations. An alternative explanation might be that latitudinal changes in phytoplankton species composition result in more virus-resistant phytoplankton species at higher latitudes, however we have no evidence to support this. We speculate that removal or inactivation rates of marine viruses by transparent exopolymer particles (TEP) might be higher at the higher latitudes (Brussaard et al. 2005b; Mari et al. 2007). TEP concentrations have been found to be correlated to phytoplankton biomass, photosynthetic activity and bacterial production (Claquin et al. 2008; Ortega-Retuerta et al. 2010), which were highest in the northern latitudes of our study (see also van de Poll et al. 2013). As fluid shear is one of the primary factors controlling aggregation in pelagic systems

4

(Jackson 1990; Malits and Weinbauer 2009), the increase of K_T with latitude might have promoted higher aggregate formation and increase the potential for viral (temporary) inactivation rates at higher latitudes.

Due to deep water formation, the North Atlantic is key to ocean circulation and global climate, absorbing ~23% of the global anthropogenic CO_2 emission (Sabine et al. 2004). Several studies predict that global warming will result in a stronger temperature stratification in the North Atlantic Ocean (Sarmiento 2004; Polovina et al. 2008), accompanied by changes in phytoplankton community structure as oligotrophic regions of the ocean expand northwards (Flombaum et al. 2013; Mojica et al. 2015). This in turn will result in alterations to virus community structure as virus populations respond to changing host distributions. Currently, grazing dominates phytoplankton mortality at higher latitudes, whereas the contribution of viral lysis is relatively small. However, our results indicate that warming of the surface layers will shift the ecosystem at high latitudes towards a more viral-lysis dominated system. The partitioning of photosynthetic carbon through these different pathways (i.e., grazing versus cell lysis) has important implications for ecosystem function as each pathway differentially affects the structure and functioning of pelagic microbial food webs. Grazing transfers carbon, nutrients and energy to higher trophic levels, thereby increasing the overall efficiency and carrying capacity of the ecosystem. In addition, the production of fecal pellets by mesozooplankton is responsible for much of the carbon transported out of the euphotic zone into the deeper ocean (Ducklow et al. 2001). Viral lysis redirects carbon and energy away from larger organisms towards the microbial loop, and thereby rapidly returns most of the organic carbon fixed by phytoplankton into the surface layer (Fuhrman 1999; Wilhelm and Suttle 1999; Brussaard et al. 2005a; Weitz and Wilhelm 2012). A more prominent role of viral lysis in the northern North Atlantic would thus markedly reduce biological carbon export into the ocean's interior in one of the key areas of global carbon sequestration, reducing the ocean's capacity to function as a long-term sink for anthropogenic carbon dioxide.

Acknowledgments

4

References

Angly FE, Felts B, Breitbart M, Salamon P, Edwards RA, Carlson C, Chan AM, Haynes M, Kelley S, Liu H, Mahaffy JM, Mueller JE, Nulton J, Olson R, Parsons R, Rayhawk S, Suttle CA, Rohwer F (2006) The marine viromes of four oceanic regions. PLOS Biology 4: e368. doi: 10.1371/journal.pbio.0040368

Baas Becking LGM (1931) Geobiologie of inleiding tot de milieukunde. W.P. Van Stockum & Zoon, the Netherlands

Baudoux AC, Noordeloos AAM, Veldhuis MJW, Brussaard CPD (2006) Virally induced mortality of *Phaeocystis globosa* during two spring blooms in temperate coastal waters. Aquatic Microbial Ecology 44: 207-217

Baudoux AC, Veldhuis MJW, Witte HJ, Brussaard CPD (2007) Viruses as mortality agents of picophytoplankton in the deep chlorophyll maximum layer during IRONAGES III. Limnology and Oceanography 52: 2519-2529

Baudoux AC, Brussaard CPD (2008) Influence of irradiance on virus-algal host interactions. Journal of Phycology 44: 902-908

Baudoux AC, Veldhuis MJW, Noordeloos AAM, van Noort G, Brussaard CPD (2008) Estimates of virus- vs. grazing induced mortality of picophytoplankton in the North Sea during summer. Aquatic Microbial Ecology 52: 69-82

Behrenfeld MJ, O 'Malley RT, Siegel DA, McClain CR, Sarmiento JL, Feldman GC, Milligan AJ, Falkowski PG, Letelier RM, Boss ES (2006) Climate-driven trends in contemporary ocean productivity. Nature 444: 752-755

Brainerd KE, Gregg MC (1995) Surface mixed and mixing layer depths. Deep-Sea Research, Part I 42: 1521-1543

Bratbak G, Jacobsen A, Heldal M, Nagasaki K, Thingstad F (1998) Virus production in *Phaeocystis pouchetii* and its relation to host cell growth and nutrition. Aquatic Microbial Ecology 16: 1-9

Bray NA, Fofonoff NP (1981) Available potential energy for mode eddies. Journal of Physical Oceanography 11: 30-47

Breitbart M, Rohwer F (2005) Here a virus, there a virus, everywhere the same virus? Trends Microbiology 13: 278-284

Brussaard CPD (2004a) Viral control of phytoplankton populations - a review. Journal of Eukaryotic Microbiology 51: 125-138

Brussaard CPD (2004b) Optimization of procedures for counting viruses by flow cytometry. Applied and Environmental Microbiology 70: 1506-1513

Brussaard CPD, Kuipers B, Veldhuis MJW (2005a) A mesocosm study of *Phaeocystis globosa* population dynamics: I. Regulatory role of viruses in bloom control. Harmful Algae 4: 859-874

Brussaard CPD, Mari X, Van Bleijswijk JDL, Veldhuis MJW (2005b) A mesocosm study of *Phaeocystis globosa* (Prymnesiophyceae) population dynamics: II. Significance for the microbial community. Harmful Algae 4: 875-893

Brussaard CPD, Martinez JM (2008) Algal bloom viruses. Plant Viruses 2: 1-13

Brussaard CPD, Payet JP, Winter C, Weinbauer M (2010) Quantification of aquatic viruses by flow cytometry. In: Wilhelm SW, Weinbauer MG, Suttle CA (eds). Manual of Aquatic Viral Ecology. ASLO

Cottrell MT, Suttle CA (1995) Dynamics of a lytic virus infecting the photosynthetic marine picoflagellate *Micromonas pusilla*. Limnology and Oceanography 40: 730-739

Daufresne M, Lengfellner K, Sommer U (2009) Global warming benefits the small in aquatic ecosystems. Proceedings of the National Academy of Sciences of the United States of America 106: 12788-12793

de Wit R, Bouvier T (2006) 'Everything is everwhere, but, the environment selects'; what did Baas Becking and Beijerinck really say? Environmental Microbiology 8: 755-758

Deser C, Blackmon ML (1993) Surface climate variations over the North Atlantic ocean during winter: 1900-1989. Journal of Climate 6: 1743-1753

Doney SC, Ruckelshaus M, Duffy JE, Barry JP, Chan F, English CA, Galindo HM, Grebmeier JM, Hollowed AB, Knowlton N, Polovina J, Rabalais NN, Sydeman WJ, Talley LD (2012) Climate change impacts on marine ecosystems. Annual Review of Marine Science 4: 11-37

Ducklow HW, Steinberg DK, Buesseler KO (2001) Upper ocean carbon export and the biological pump. Oceanography 14: 50-58

Edwards M, Richardson AJ (2004) Impact of climate change on marine pelagic phenology and trophic mismatch. Nature 430: 881-884

Evans C, Archer SD, Jacquet S, Wilson WH (2003) Direct estimates of the contribution of viral lysis and microzooplankton grazing to the decline of a *Micromonas* spp. population. Aquatic Microbial Ecology 30: 207-219

Evans C, Brussaard CPD (2012) Viral lysis and microzooplankton grazing of phytoplankton throughout the Southern Ocean. Limnology and Oceanography 57: 1826-1837

Field CB, Behrenfeld MJ, Randerson JT, Falkowski P (1998) Primary production of the biosphere: Integrating terrestrial and oceanic components. Science 281: 237-240

Flombaum P, Gallegos JL, Gordillo RA, Rincon J, Zabala LL, Jiao N, Karl DM, Li WKW, Lomas MW, Veneziano D, Vera CS, Vrugt JA, Martiny AC (2013) Present and future global distributions of the marine cyanobacteria *Prochlorococcus* and *Synechococcus*. Proceedings of the National Academy of Sciences of the United States of America 110: 9824-9829

Franks PJS (2001) Phytoplankton blooms in a fluctuating environment: the roles of plankton response time scales and grazing. Journal of Plankton Research 23: 1433-1441

Fuhrman JA (1999) Marine viruses and their biogeochemical and ecological effects. Nature 399: 541-548

Fuhrman JA, Steele JA, Hewson I, Schwalbach MS, Brown MV, Green JL, Brown JH (2008) A latitudinal diversity gradient in planktonic marine bacteria. Proceedings of the National Academy of Sciences of the United States of America 105: 7774-7778

Furrer R, Nychka D, Sain S (2012) fields: Tools for spatial data. R package version 6.7: http://CRAN.R-project.org/package=fields

Gobler CJ, Hutchins DA, Fisher NS, Cosper EM, Sanudo-Wilhelmy SA (1997) Release and bioavailability of C, N, P, Se, and Fe following viral lysis of a marine chrysophyte. Limnology and Oceanography 42: 1492-1504

Grasshoff K (1983) Determination of nitrate. In: Grasshoff K, Erhardt M, Kremeling K (eds) Methods of Seawater Analysis. Verlag Chemie: Weinheim, Germany

Gregg WW, Conkright ME, Ginoux P, O 'Reilly JE, Casey NW (2003) Ocean primary production and climate: global decadal changes. Geophysical Research Letters 30: 1809. doi:10.1029/2003GL016889

Haaber J, Middelboe M (2009) Viral lysis of *Phaeocystis pouchetii*: Implications for algal population dynamics and heterotrophic C, N and P cycling. The ISME Journal 3: 430-441

Helder W, de Vries RTP (1979) An automatic phenol-hypochlorite method for the determination of ammonia in sea and brackish water. Netherlands Journal of Sea Research 13: 154-160

Hilligsøe KM, Richardson K, Bendtsen J, Sorensen LL, Nielsen TG, Lyngsgaard MM (2011) Linking phytoplankton community size composition with temperature, plankton food web structure and sea-air CO_2 flux. Deep-Sea Research, Part I 58: 826-838

Huisman J, van Oostveen P, Weissing FJ (1999) Critical depth and critical turbulence: two different mechanisms for the development of phytoplankton blooms. Limnology and Oceanography 44: 1781-1787

Huisman J, Sharples J, Stroom JM, Visser PM, Kardinaal WEA, Verspagen JMH, Sommeijer B (2004) Changes in turbulent mixing shift competition for light between phytoplankton species. Ecology 85: 2960-2970

Huisman J, Thi NNP, Karl DM, Sommeijer B (2006) Reduced mixing generates oscillations and chaos in the oceanic deep chlorophyll maximum. Nature 439: 322-325

Irigoien X, Huisman J, Harris RP (2004) Global biodiversity patterns of marine phytoplankton and zooplankton. Nature 429: 863-867

Jackson GA (1990) A model of the formation of marine algal flocs by physical coagulation processes. Deep-Sea Research, Part A 37: 1197-1211

Jacquet S, Heldal M, Iglesias-Rodriguez D, Larsen A, Wilson W, Bratbak G (2002) Flow cytometric analysis of an *Emiliana huxleyi* bloom terminated by viral infection. Aquatic Microbial Ecology 27: 111-124

4

Jurado E, van der Woerd HJ, Dijkstra HA (2012) Microstructure measurements along a quasi-meridional transect in the northeastern Atlantic Ocean. Journal of Geophysical Research 117: C04016. doi: 10.1029/2011JC007137

Keller DP, Hood RR (2011) Modeling the seasonal autochthonous sources of dissolved organic carbon and nitrogen in the upper Chesapeake Bay. Ecological Modelling 222: 1139-1162

Keller DP, Hood RR (2013) Comparative simulations of dissolved organic matter cycling in idealized oceanic, coastal, and estuarine surface waters. Journal of Marine Systems109: 109-128

Kimmance SA, Wilson WH, Archer SD (2007) Modified dilution technique to estimate viral versus grazing mortality of phytoplankton: limitations associated with method sensitivity in natural waters. Aquatic Microbial Ecology 49: 207-222

Kimmance SA, Brussaard CPD (2010) Estimation of viral-induced phytoplankton mortality using the modified dilution method. In: Wilhelm SW, Weinbauer M, Suttle CA (eds) Manual of Aquatic Viral Ecology. ASLO

Koroleff F (1969) Direct determination of ammonia in natural waters as indophenol blue. Coun. Meet. int. Coun. Explor. Sea **C.M.-ICES/C:** 9

Levitus S, Antonov JI, Boyer TP, Stephens C (2000) Warming of the world ocean. Science 287: 2225-2229

Longhurst AR (2007) Ecological Geography of the Sea. Academic Press, London

Maat DS, Crawfurd KJ, Timmermans KR, Brussaard CPD (2014) Elevated partial CO_2 pressure and phosphate limitation favor *Micromonas pusilla* through stimulated growth and reduced viral impact. Applied and Environmental Microbiology 80: 3119-3127

Malits A, Weinbauer MG (2009) Effect of turbulence and viruses on prokaryotic cell size, production and diversity. Aquatic Microbial Ecology 54: 243-254

Mari X, Kerros ME, Weinbauer MG (2007) Virus attachment to transparent exopolymeric particles along trophic gradients in the southwestern lagoon of New Caledonia. Applied and Environmental Microbiology 73: 5245-5252

Marie D, Brussaard CPD, Thyrhaug R, Bratbak G, Vaulot D (1999) Enumeration of marine viruses in culture and natural samples by flow cytometry. Applied and Environmental Microbiology 65: 45-52

Marie D, Simon N, Vaulot D (2005) Phytoplankton cell counting by flow cytometry. In: Andersen RA (ed) Algal culturing techniques. Elsevier Academic Press, Burlington

Martiny JBH, Bohannan BJM, Brown JH, Colwell RK, Fuhrman JA, Green JL, Horner-Devine MC, Kane M, Krumins JA, Kuske CR, Morin PJ, Naeem S, Ovreas L, Reysenbach AL, Smith VH, Staley JT (2006) Microbial biogeography: putting microorganisms on the map. Nature Reviews Microbiology 4: 102-112

Matteson AR, Loar SN, Pickmere S, DeBruyn JM, Ellwood MJ, Boyd PW, Hutchins DA, Wilhelm SW (2012) Production of viruses during a spring phytoplankton bloom in the South Pacific Ocean near of New Zealand. FEMS Microbiology Ecology 79: 709-719

Matteson AR, Rowe JM, Ponsero AJ, Pimentel TM, Boyd PW, Wilhelm SW (2013) High abundances of cyanomyoviruses in marine ecosystems demonstrate ecological relevance. FEMS Microbiology Ecology 84: 223-234

Mitra A, Flynn KJ (2005) Predator-prey interactions: is 'ecological stoichiometry' sufficient when good food goes bad? Journal of Plankton Research 27: 393-399

Moebus K (1996) Marine bacteriophage reproduction under nutrient-limited growth of host bacteria. I. Investigations with six phage-host systems. Marine Ecology Progress Series 144: 1-12

Mojica KDA, Brussaard CPD (2014) Factors affecting virus dynamics and microbial host-virus interactions in marine environments. FEMS Microbiology Ecology 89: 495-515

Mojica KDA, Evans C, Brussaard CPD (2014) Flow cytometric enumeration of marine viral populations at low abundances. Aquatic Microbial Ecology 71: 203-209

Mojica KDA, van de Poll WH, Kehoe M, Huisman J, Timmermans KR, Buma AGJ, van der Woerd HJ, Hahn-Woernle L, Dijkstra HA, Brussaard CPD (2015). Phytoplankton community structure in relation to vertical stratification along a north-south gradient in the Northeast Atlantic Ocean. Limnology and Oceanography (in press). doi: 10.1002/lno.10113

Mühling M, Fuller NJ, Millard A, Somerfield PJ, Marie D, Wilson WH, Scanlan DJ, Post AF, Joint I, Mann NH (2005) Genetic diversity of marine *Synechococcus* and co-occurring cyanophage communities: evidence for viral control of phytoplankton. Environmental Microbiology 7: 499-508

Murphy J, Riley JP (1962) A modified single solution method for the determination of phosphate in natural waters. Analytica Chimica Acta 27: 31-36

Nagasaki K, Yamaguchi M (1998) Effect of temperature on the algicidal activity and the stability of HaV (*Heterosigma akashiwo* virus). Aquatic Microbial Ecology 15: 211-216

Oksanen J, Blanchet FG, Kindt R, Legendre P, Minchin PR, O'Hara RB, Simpson GL, Solymos, P, Stevens MHH, Wagner H (2013) vegan: Community ecology package. http://CRAN.R-project.org/package=vegan

Paul JH (2008) Prophages in marine bacteria: dangerous molecular time bombs or the key to survival in the seas? The ISME Journal 2: 579-589

Polovina JJ, Howell EA, Abecassis M (2008) Ocean's least productive waters are expanding. Geophysical Research Letters 35: L03618. doi: 10.1029/2007GL031745

R Development Core Team (2012) R: A language and environment for statistical computing. R Foundation for Statistical Computing: Vienna, Austria, ISBN 3-900051-07-0, http://www.R-project.org

Revelle W (2014) psych: Procedures for Psychological, Psychometric, and Personality Research. R Package Version 1.4.5. http://CRAN.R-project.org/package=psych

Richardson AJ, Schoeman DS (2004) Climate impact on plankton ecosystems in the Northeast Atlantic. Science 305: 1609-1612

Sabine CL, Feely RA, Gruber N, Key RM, Lee K, Bullister JL, Wanninkhof R, Wong CS,

Wallace DWR, Tilbrook B, Millero FJ, Peng T-H, Kozyr A, Ono T, Rios AF (2004) The oceanic sink for anthropogenic CO_2. Science 305: 367-371

Sarmiento JL, Hughes TMC, Stouffer RJ, Manabe S (1998) Simulated response of the ocean carbon cycle to anthropogenic climate warming. Nature 393: 245-249

Sarmiento JL (2004) Response of ocean ecosystems to climate warming. Global Biogeochemical Cycles 18: GB3003. doi: 10.1029/2003GB002134

Scanlan DJ, West NJ (2002) Molecular ecology of the marine cyanobacterial genera *Prochlorococcus* and *Synechococcus*. FEMS Microbiology Ecology 40: 1-12

Schlitzer R (2002) Interactive analysis and visualization of geoscience data with Ocean Data View. Computers and Geosciences 28: 1211-1218

Siegel DA, Doney SC, Yoder JA (2002) The North Atlantic spring phytoplankton bloom and Sverdrup's critical depth hypothesis. Science 296: 730-733

Stevens C, Smith M, Ross A (1999) SCAMP: measuring turbulence in estuaries, lakes, and coastal waters. NIWA - Water Atmosphere 7: 20-21

Suttle CA, Chan AM, Cottrell MT (1990) Infection of phytoplankton by viruses and reduction of primary productivity. Nature 347: 467-469

Suttle CA, Chan AM (1993) Marine cyanophages infecting oceanic and coastal strains of *Synechococcus*: abundance, morphology, cross-infectivity and growth characteristics. Marine Ecology Progress Series 92: 99-109

Suttle CA, Chan AM (1994) Dynamics and distribution of cyanophages and their effect on marine *Synechococcus* spp. Applied and Environmental Microbiology 60: 3167-3174

Suttle CA (2007) Marine viruses - major players in the global ecosystem. Nature Reviews 5: 801-812

Sverdrup, EU (1953) On conditions for the vernal blooming of phytoplankton. Journal du Conseil / Conseil Permanent International pour l'Exploration de la Mer 18: 287-295

Taylor JR, Ferrari R (2011) Shutdown of turbulent convection as a new criterion for the onset of spring phytoplankton blooms. Limnology and Oceanography 56: 2293-2307

Thingstad TF, Våge S, Storesund JE, Sandaa R-A, Giske J (2014) A theoretical analysis of how strain-specifc viruses can control microbial species diversity. Proceedings of the National Academy of Sciences of the United States of America 111: 7813-7818

4

Toggweiler JR, Russell J (2008) Ocean circulation in a warming climate. Nature 451: 286-288

Tomaru Y, Tarutani K, Yamaguchi M, Nagasaki K (2004) Quantitative and qualitative impacts of viral infection on a *Heterosigma akashiwo* (Raphidophyceae) bloom in Hiroshima Bay, Japan. Aquatic Microbial Ecology 34: 227-238

Tsai AY, Gong GC, Sanders RW, Chiang KP, Huang JK, Chan YF (2012) Viral lysis and nanoflagellate grazing as factors controlling diel variations of *Synechococcus* spp. summer abundance in coastal waters of Taiwan. Aquatic Microbial Ecology 66: 159-167

van de Poll WH, Kulk G, Timmermans KR, Brussaard CPD, van der Woerd HJ, Kehoe MJ. Mojica KDA, Visser RJW, Rozeman PD, Buma AGJ (2013) Phytoplankton chlorophyll *a* biomass, composition, and productivity along a temperature and stratification gradient in the northeast Atlantic Ocean. Biogeosciences 10: 4227-4240

van de Waal DB, Verschoor AM, Verspagen JMH, Van Donk E, Huisman J (2010) Climate-driven changes in the ecological stoichiometry of aquatic ecosystems. Frontiers in Ecology and the Environment 8: 145-152

Van Etten JL, Burbank DE, Xia Y, Meints RH (1983) Growth cycle of a virus, PBCV-1, that infects Chlorella-like algae. Virology 126: 117-125

Wang K, Wommack KE, Chen F (2011) Abundance and distribution of Synechococcus spp. and cyanophages in the Chesapeake Bay. Applied and Environmental Microbiology 77: 7459-7468

Waterbury JB, Valois FW (1993) Resistance to co-occurring phages enables marine *Synechococcus* communities to coexist with cyanophages abundant in seawater. Applied and Environmental Microbiology 59: 3393-3399

Weitz JS, Wilhelm SW (2012) Ocean viruses and their effects on microbial communities and biogeochemical cycles. F1000 Biology Reports 4

Wilhelm SW, Suttle CA (1999) Viruses and nutrient cycles in the sea - Viruses play critical roles in the structure and function of aquatic food webs. Bioscience 49: 781-788

Wilson WH, Nicholas JF, Joint IR, Mann NH (1999) Analysis of cyanophage diversity and population structure in a south-north transect of the Atlantic Ocean. Bulletin of the Institute of Oceanography and Fisheries 19: 209-216

Yang YH, Motegi C, Yokokawa T, Nagata T (2010) Large-scale distribution patterns of virioplankton in the upper ocean. Aquatic Microbial Ecology 60: 233-246

Zuur A, Ieno EN, Walker N, Saveliev AA, Smith GM (2009) Mixed Effects Models and Extensions in Ecology with R. Springer, New York

Zuur AF, Ieno EN, Elphick CS (2010) A protocol for data exploration to avoid common statistical problems. Methods in Ecology and Evolution 1: 3-14

Supporting information

Table S1. Location and physicochemical characteristics of water sampled in the North Atlantic for modified dilution experiments during the STRATIPHYT and MEDEA cruises. Abbreviations for depth layer are mixed layer (ML) and deep chlorophyll maximum (DCM).

Cruise	Experiment No.	Station	Latitude (°N)	Longitude (°E)	Depth (m)	Depth Layer	Temperature (°C)	Salinity	Sigma-t	PO_4^{3-} (µM)	NO_x (µM)	NO_2^- (µM)	NH_4^+ (µM)
STRATIPHYT	1	0	29.000	-15.000	80	DCM	19.0	36.8	26.8	0.02	0.02	0.01	0.07
STRATIPHYT	2	1	30.018	-15.071	74	DCM	18.2	36.7	26.8	0.03	0.11	0.09	0.06
STRATIPHYT	3	3	32.825	-14.589	57	DCM	18.0	36.5	26.7	0.00	0.15	0.02	0.06
STRATIPHYT	4	5	34.720	-14.258	85	DCM	16.3	36.3	27.0	0.04	0.15	0.06	0.15
STRATIPHYT	5	7	36.526	-13.934	75	DCM	16.1	36.3	27.0	0.02	0.11	0.00	0.08
STRATIPHYT	6	11	40.528	-13.191	55	DCM	15.2	36.0	26.9	0.04	0.03	0.03	0.07
STRATIPHYT	7	13	42.337	-12.884	47	DCM	14.7	35.8	26.9	0.05	0.10	0.01	0.00
STRATIPHYT	8	15	44.283	-12.605	60	DCM	14.4	35.8	27.0	0.17	2.21	0.16	0.07
STRATIPHYT	9	17	45.526	-12.426	50	DCM	14.2	35.7	26.9	0.10	1.15	0.09	0.13
STRATIPHYT	10	19	49.382	-11.829	15	ML	15.8	35.5	26.3	0.12	1.18	0.04	0.36
STRATIPHYT	11	24	55.713	-14.278	20	ML	13.9	35.3	26.6	0.20	2.71	0.13	0.09
STRATIPHYT	12	25	58.002	-16.516	10	ML	13.5	35.3	26.6	0.11	1.18	0.05	0.09
STRATIPHYT	13	27	59.499	-18.067	20	ML	14.0	35.2	26.5	0.18	2.11	0.03	0.19
STRATIPHYT	14	29	60.684	-19.339	10	ML	13.0	35.3	26.6	0.19	2.07	0.09	0.14
STRATIPHYT	15	30	61.712	-20.485	10	ML	13.2	35.2	26.6	0.13	1.02	0.02	0.24
MEDEA	16	2	45.150	-13.700	45	DCM	17.5	35.8	26.0	0.08	0.61	0.13	
MEDEA	17	3	47.360	-15.930	35	DCM	16.5	35.7	26.2	0.06	0.14	0.05	
MEDEA	18	4	48.000	-18.890	35	ML	16.4	35.7	26.2	0.06	0.14	0.04	
MEDEA	19	6	46.080	-21.310	52	ML	15.2	35.8	26.6	0.24	3.34	0.30	
MEDEA	20	7	42.560	19.550	70	DCM	15.8	36.0	26.6				
MEDEA	21	8	39.900	-20.470	77	DCM	16.4	36.2	26.6	0.04	0.47	0.09	
MEDEA	22	9	37.660	-21.400	86	DCM	17.2	36.3	26.5	0.02	0.14	0.03	
MEDEA	23	10	35.900	-23.830	85	DCM	15.9	36.2	26.7	0.12	1.82	0.14	
MEDEA	24	11	33.930	-26.610	90	DCM	19.3	36.7	26.2	0.01	0.07	0.04	

4

Table S1. Continued.

Cruise	Experiment No.	Station	Latitude (°N)	Longitude (°E)	Depth (m)	Depth Layer	Temperature (°C)	Salinity	Sigma-t	PO$_4^{3-}$ (µM)	NO$_x$ (µM)	NO$_2^-$ (µM)	NH$_4^+$ (µM)
MEDEA	25	13	30.460	-32.210	100	DCM	19.2	36.7	26.3	0.01	0.02	0.01	
MEDEA	26	15	26.060	-36.120	120	DCM	21.1	37.1	26.1	0.02	0.10	0.06	
MEDEA	27	16	24.670	-34.940	116	DCM	21.6	37.2	26.0	0.01	0.04	0.03	
MEDEA	28	17	25.580	-32.270	121	DCM	20.7	37.1	26.2				
MEDEA	29	18	27.100	-29.820	108	DCM	21.2	37.2	26.1	0.01	0.03	0.01	
MEDEA	30	19	28.540	-27.460	106	DCM	19.7	36.8	26.3	0.02	0.05	0.01	
MEDEA	31	20	30.460	-24.500	103	DCM	19.7	36.8	26.3	0.01	0.03	0.02	
MEDEA	32	21	32.090	-22.420	100	DCM	18.7	36.6	26.3	0.01	0.06	0.01	
MEDEA	33	22	31.030	-20.090	93	DCM	18.5	36.6	26.4	0.02	0.08	0.02	
MEDEA	34	24	32.250	-13.580	84	DCM	19.3	36.5	26.1	0.01	0.03	0.01	

Table S2. Abundance (P0; 103 cells mL-1) and the rates (d-1) of gross growth (µgross), total mortality (TM), grazing (G) and viral lysis (V) of different phytoplankton groups sampled in the North Atlantic modified dilution experiments conducted during the STRATIPHYT and MEDEA cruises.

Experiment No.	Synechococcus					Prochlorococcus LL					Pico I					Pico II				
	P0	µgross	TM	G	V	P0	µgross	TM	G	V	P0	µgross	TM	G	V	P0	µgross	TM	G	V
1	17.0	0.43*	0.04	0.00	0.04	136	0.18*	0.31*	0.14	0.17	30.0	0.12*	0.39*	0.25*	0.14	2.4	0.36*	0.35*	0.03	0.31
2	64.5	0.20*	0.28*	0.17*	0.11											5.8	0.41*	0.40*	0.18	0.21
3																0.8	0.92*	0.75*	0.60*	0.15
4	1.7	0.62*	0.71*	0.22	0.49*	65	0.60*	0.74*	0.17	0.57*	1.3	0.56*	0.72*	0.21	0.52*	0.8	1.15*	1.01*	0.24	0.77*
5	5.3	0.23*	0.29*	0.23*	0.06	113	0.26*	0.43*	0.25*	0.18	2.2	0.37*	0.42*	0.18	0.25	3.4	0.42*	0.43*	0.23*	0.19
6						112	0.08*	0.13*	0.09*	0.03	5.1	0.07*	0.13*	0.01	0.12*					
7																2.8	0.07*	0.41*	0.37*	0.04
8	5.9	0.35*	0.29*	0.22*	0.07	21	0.33*	0.38*	0.27*	0.11	4.7	0.42*	0.27*	0.05	0.22	4.0	0.43*	0.46	0.21*	0.25
9	10.3	0.32*	0.44*	0.00	0.44*	44	0.34*	0.50*	0.09	0.41*	4.8	0.60*	0.49*	0.10	0.40*	4.7	-0.13	0.41*	0.14	0.26
10											1.9	0.17	0.17	0.11	0.06	7.9	0.20*	0.08	0.00	0.08
11	3.3	0.41*	0.52*	0.30*	0.22*						2.0	0.44*	0.85*	0.60	0.25	16.1	0.26*	0.47*	0.24*	0.23
12																11.5	0.26*	0.16	0.16*	0.00
13	43.9	0.34*	0.43*	0.35*	0.08						6.0	0.33*	0.56*	0.56*	0.01	6.4	0.38*	0.39*	0.38*	0.01
14	72.3	0.41*	0.33*	0.23*	0.10						6.6	0.59*	0.36*	0.35	0.02	4.3	0.65*	0.53*	0.45	0.07
15											7.1	0.11	0.14	0.12	0.02	6.4	0.24*	0.06	0.03	0.02
16	9.4	0.18*	0.27*	0.12*	0.15*	75	0.12*	0.20*	0.13	0.07						2.5	0.00	0.32*	0.10*	0.21*
17	25.2	0.15*	0.22*	0.17*	0.05											3.9	-0.02	0.14*	0.12	0.02
18	25.2	0.10*	0.08	0.07*	0.01	47	0.19*	0.12*	0.08	0.04	2.2	0.14*	0.11	0.09	0.02	4.6	0.13	0.10	0.00	0.10
19	3.8	0.04*	0.19*	0.05	0.14	122	-0.04*	0.19*	0.15	0.04										
20	3.9	0.08*	0.17*	0.04	0.13															
21	0.3	0.26*	0.10	0.07	0.03											1.1	0.09*	0.14*	0.07	0.07
22	0.6	0.12*	0.14	0.01	0.13						0.9	0.02	0.23*	0.20	0.03	1.8	0.16*	0.31*	0.00	0.31*
23																0.9	0.18*	0.11	0.00	0.11
24						91	-0.01	0.14*	0.08*	0.07	0.1	0.26	0.63	0.26	0.37	0.8	0.19	0.30	0.12	0.18

4

25
Table S2. Continued.

Experiment No.	Synechococcus					Prochlorococcus LL					Pico I					Pico II				
	P_0	μ_{gross}	T_M	G	V	P_0	μ_{gross}	T_M	G	V	P_0	μ_{gross}	T_M	G	V	P_0	μ_{gross}	T_M	G	V
26											0.2	0.16	0.38	0.24	0.13					
27											0.1	0.97*	0.68	0.56	0.12					
28											0.3	-0.23	1.07*	0.02	1.05*					
29	0.3	0.26*	0.31	0.07	0.25											0.5	0.22*	0.41*	0.10	0.31*
30																0.5	0.16*	0.20*	0.06	0.15
31																0.8	0.09	0.00	0.00	0.00
32						48	0.10*	0.08	0.05	0.02	0.1	0.55*	1.06*	0.39	0.67					
33	0.5	0.41*	0.34*	0.20	0.14	80	0.27*	0.23*	0.21*	0.02						0.6	0.29*	0.30*	0.25	0.05
34	3.7	0.54*	0.13	0.03	0.10	99	0.38*	0.05	0.00	0.05										

Footnotes: *Significant results α<0.10; viral lysis rates are only signified as significant when the interaction term between grazing and grazing + viral lysis regressions was significant.

Table S2. Continued.

Experiment No.	Nano I					Nano II					Nano III				
	P_0	μ_{gross}	T_M	G	V	P_0	μ_{gross}	T_M	G	V	P_0	μ_{gross}	T_M	G	V
1	0.2	0.37	0.95*	0.77	0.18										
2															
3	0.1	0.88*	0.84*	0.67*	0.17										
4	0.2	0.79*	1.20*	0.31	0.89*										
5	1.0	0.44*	0.53*	0.26	0.27										
6	0.7	0.57*	0.33*	0.19	0.14	0.3	0.50*	0.31	0.19	0.13					
7															
8	0.5	1.08*	0.94*	0.22	0.71										
9	0.8	0.31*	0.55*	0.16	0.39										
10															
11	2.2	-0.06	0.28*	0.00	0.28	0.2	0.01	0.16	0.04	0.13	0.1	1.01*	0.54	0.38	0.17
12	1.8	1.03*	0.52*	0.12	0.41						0.4	0.68*	0.50	0.08	0.42
13	2.4	0.89*	0.66*	0.51*	0.15	0.1	1.36*	0.94*	0.36	0.59	0.5	0.68*	0.54*	0.50	0.03
14	1.2	0.86*	0.75*	0.75*	0.00						0.1	0.48	0.26	0.11	0.15
15	1.5	0.46*	0.05	0.05	0.00						0.3	0.61*	0.41	0.35	0.06
16	0.5	-0.41	0.16	0.00	0.16										
17	1.1	-0.21*	0.19*	0.00	0.19										
18															
19	1.1	0.00	0.32*	0.02	0.29										
20															
21															
22															
23	0.1	-0.04	0.05	0.00	0.05										
24															
25	0.3	-0.42*	0.26	0.07	0.19										

Table S2. Continued.

4

Experiment No.	Nano I					Nano II					Nano III				
	P_0	μ_{gross}	T_M	G	V	P_0	μ_{gross}	T_M	G	V	P_0	μ_{gross}	T_M	G	V
26															
27															
28															
29															
30															
31															
32															
33															
34	0.3	0.32*	0.40*	0.20	0.20										

Table S3. Spearman rank correlation coefficients (above the diagonal) and associated p-values (below the diagonal with significant values highlighted in bold) relating virus abundance data to the viral lysis rate obtained from modified dilution assays conducted during the STRATIPHYT cruise (N = 64). Abbreviations represent viral lysis rate (VL), abundances of individual virus populations (V1 - V5), total virus abundance (Total V) and the ratio of viral lysis to grazing rate (V:G).

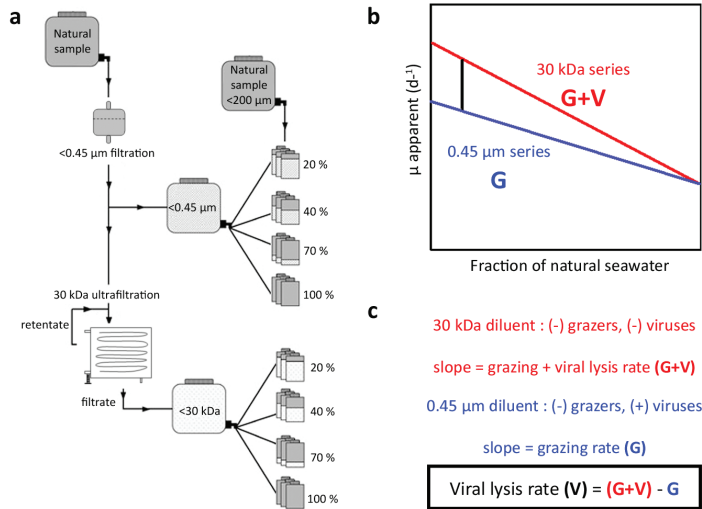|	Latitude	VL	V1	V2	V3	V4	V5	Total V	V:G
Latitude		-0.60	0.70	0.72	-0.72	n.s.	n.s.	0.75	-0.54
VL	**0.00**		-0.63	-0.44	0.42	n.s.	n.s.	-0.66	0.81
V1	**0.00**	**0.00**		0.80	-0.51	n.s.	0.68	0.99	-0.61
V2	**0.00**	**0.03**	**0.00**		n.s.	n.s.	0.75	0.85	n.s.
V3	**0.00**	**0.05**	**0.00**	0.07		n.s.	n.s.	-0.53	0.43
V4	1.00	1.00	1.00	1.00	1.00		0.47	n.s.	n.s.
V5	0.19	0.11	**0.00**	**0.00**	0.23	**0.01**		0.69	n.s.
Total V	**0.00**	**0.00**	**0.00**	**0.00**	**0.00**	1.00	**0.00**		-0.61
V:G	**0.00**	**0.00**	**0.00**	0.75	**0.05**	1.00	1.00	**0.00**	

n.s. indicates non-significance at α = 0.05

4

Figure S1. (**a**) Experimental set-up of the modified dilution method for estimating loss rates of natural phytoplankton populations. Filtered samples are mixed with unfiltered samples ("natural water") at different proportions. Filtration < 0.45 µm removes microzooplankton but not viruses; filtration < 30 kDa removes both microzooplankton and viruses. (**b**) Illustration of the typical regression lines which result from plotting phytoplankton growth after 24 hour incubation under in situ light and temperature (µ apparent) versus the fraction of natural water. (**c**) Explanation for the determination of viral lysis rates (V) and microzooplankton grazing rates (G) using regression analysis. Figure adapted from Baudoux et al. (2006).
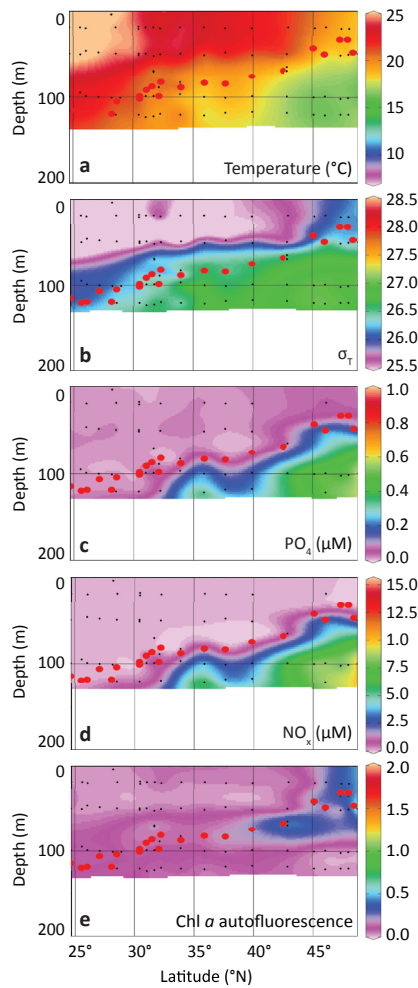
Figure S2. Latitudinal and depth distribution of (**a**) temperature, (**b**) sigma-t (σ_T), (**c**) inorganic phosphorus, (**d**) NO_x (nitrate + nitrite) and (**e**) Chl *a* autofluorescence measured during MEDEA. Black dots indicate sampling points and red dots the sampling depths for modified dilution assays. Figure panels were prepared using Ocean Data View (ODV version 4.6.5, Schlitzer, 2002).
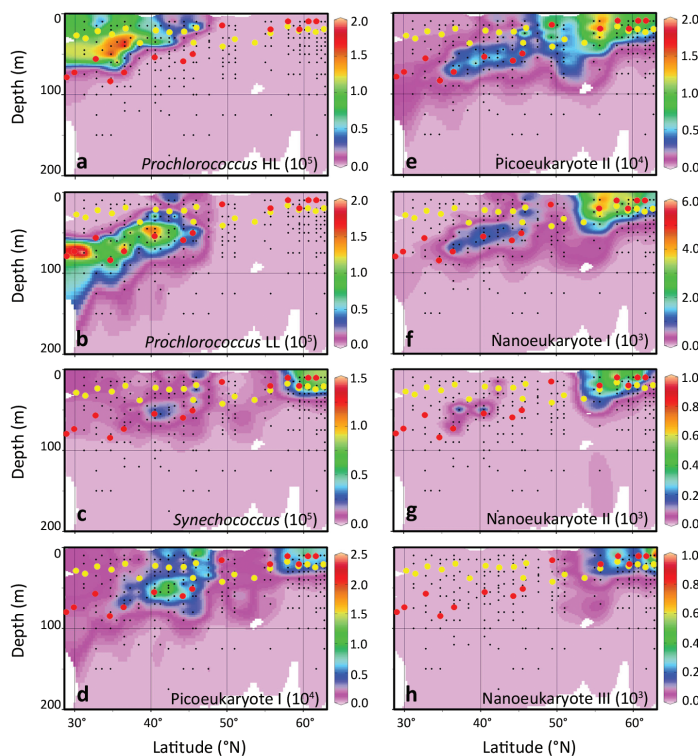
Figure S3. Biogeographical distributions of main phytoplankton groups across the Northeast Atlantic Ocean. (**a**) Prochlorococcus, high-light adapted phenotypes (0.4-0.8 μm Ø) (cells ml^{-1}). (**b**) Prochlorococcus, low-light adapted phenotypes (0.4-1.0 μm Ø) (cells ml^{-1}). (**c**) Synechococcus spp. (0.8-1.5 μm Ø) (cells ml^{-1}). (**d-e**) photosynthetic picoeukaryotes, group I (0.8-2.0 μm Ø) and group II (1-2 μm Ø) (cells ml^{-1}). (**f-h**) photosynthetic nanoeukaryotes, group I (2-5 μm Ø), group II (3-8 μm Ø), group III (5-10 μm Ø) (cells ml^{-1}). Data were obtained by flow cytometry during the STRATIPHYT cruise. Black dots indicate sampling points, yellow dots indicate mixed layer depth (Z_m), and red dots the sampling depths for modified dilution assays. Graphs were prepared with Ocean Data View (ODV version 4.6.5, Schlitzer, 2002).